Flame Length Scaling of C₂H₄-Air Premixed Flames under Acoustic Forcing

D. Hwang[1], K. Ahn[1†] and Y. Yoon[2]

[1] *School of Mechanical Engineering, Chungbuk National University, Chungdae-ro 1, Seowon-gu, Cheongju, Chungbuk 28644, Korea*
[2] *Department of Aerospace Engineering, Seoul National University, 1 Gwanak-ro, Gwanak-gu, Seoul 08826, Korea*

†*Corresponding Author Email: kbahn@cbnu.ac.kr*

ABSTRACT

An experimental study has been carried out to investigate the effects of inlet velocity, equivalence ratio, and acoustic forcing on flame lengths and flame center lengths in a dump combustor. A premixed gas of ethylene and air was supplied to a combustor through an inlet section and an acoustic driver was used to generate acoustic forcing to simulate unstable combustion. By changing these parameters, combustion tests were performed and flame images were taken using an ICCD camera with a bandpass filter corresponding to a CH* chemiluminescence band. Flame lengths/flame center lengths were obtained from the flame images and were analyzed with respect to dimensional parameters. For a more general finding, the flame length and flame center length were normalized by the inlet width. The dimensional parameters were also replaced with non-dimensional parameters such as the Reynolds number, Strouhal number, Damköhler number, and normalized inlet velocity fluctuation, since dimensional parameters have a complex influence on these non-dimensional parameters. The normalized flame lengths and flame center lengths could be expressed well as a function of the non-dimensional parameters. It was found that an increase in the Reynolds number and a decrease in the Strouhal number, Damköhler number and normalized inlet velocity fluctuation caused the flame length/flame center length to become greater.

1. INTRODUCTION

Since the flame length is a dominant factor in the combustion efficiency, heat release/transfer, and NOx formation in dump combustors of gas turbine engines and ramjet engines, it has been a subject of great importance to many researchers (Bondaryuk and Il'yashenko 1960; Hill and Peterson 1992; Turns 2012). The flame length in premixed and non-premixed turbulent flames is affected by the geometric dimensions of a combustor and the operating conditions, such as the inlet velocity/temperature, equivalence ratio, combustion pressure, etc. (Dahm and Mayman 1990; Morcos and Abdel-Rahim 1999; Choi and Kim 2002).

Gas turbine engines are generally designed to work at low equivalence ratios to reduce NOX formation due to strict emission regulations (Lefebvre 1977; Foglesong *et al.* 1999; Lieuwen and Yang 2005) and ramjet engines are operated in the vicinity of a stoichiometric condition to increase the combustion efficiency (Bondaryuk and Il'yashenko 1960).

Combustion instabilities, with high pressure fluctuations, are often encountered in these operating regions, and large-scale coherent vortical structures are known to play a critical role in sustaining such combustion instabilities. Poinsot *et al.* (1987) proposed various mechanisms for low-frequency vortex-driven instabilities. Yu *et al.* (1991) showed that both the vortex kinetics in the combustor and acoustic response of the inlet section control the instability frequency. Byrne (1983) concentrated on the relationship between the flow dynamics observed in acoustically excited jets and ramjet pressure oscillations. Altay *et al.* (2009a) discovered four distinct operating modes for the combustor depending on experimental conditions. Dhanuka *et al.* (2011) found that the frequency of a lean-limit instability is related to the flow velocity, flame velocity, and combustor length.

Previous research has shown that acoustic forcing in premixed flames and non-premixed flames causes heat release patterns to periodically change and a high heat release region to be distributed in the near

field of the combustor (Ahn and Yu 2012; Kim *et al.* 2009a). Hot-firing tests in combustors, using kerosene and liquid oxygen for a liquid rocket engine, also indicated that low-frequency combustion instabilities induced the high temperature region to move forward near the faceplate plane of the combustor and high-frequency combustion instabilities also increased heat flux into the combustion chamber by 5 ~ 20% (Ahn 2014; Ahn *et al.* 2014).

Several numerical simulations and experiments have shown that reaction zones in the vortex structure are affected by flow conditions such as the Strouhal number and the Damköhler number (Ghoniem and Heidarinejad 1991; Rutland and Ferziger 1991; Renard *et al.* 2000; Stöhr *et al.* 2013). The zone of heat release could be moved further downstream of the vortex structure under low Damköhler numbers. Buchner *et al.* (1993) found that the dynamic behavior of jet flames was predominantly a function of the Strouhal number. Combustion instability changes the flame length and the flame center length, and therefore the heat release pattern, which affects heat transfer to the chamber walls (Ahn 2014; Kim and Santavicca 2009). A study on the flame length and flame center length in unstable combustion is therefore very important. Though numerous numerical and experimental works have been performed, a parametric study focusing on the flame length and flame center length in a dump combustor with unstable combustion has not been reported.

The first objective of the present study is to investigate the effects of inlet velocity, equivalence ratio and acoustic forcing frequency/amplitude on flame lengths and flame center lengths in a dump combustor simulating unstable combustion. The second objective is then to examine whether flame lengths and flame center lengths can be expressed as a function of non-dimensional parameters such as the Reynolds number, Strouhal number, Damköhler number, and normalized inlet velocity fluctuation. If one estimates the flame length and flame center length by knowing the non-dimensional parameters, it will help to understand and predict combustion instabilities in gas turbine engines and ramjet engines.

2. EXPERIMENTAL METHODS

2.1 Experimental Set-up

The experimental apparatus for the model dump combustor is as shown in Fig. 1. The inlet section had a cross section of 25×25 mm and a length of 360 mm. Ethylene (C_2H_4) and air were supplied into the inlet section at a height of 35 mm from the bottom. The flow rates were controlled using choked orifice nozzles (O'Keefe Controls Co.), which were located opposite one another on the side walls. A honeycomb was installed in the inlet to straighten out the premixed flow. The combustor section had a cross section of 25×75 mm and a length of 270 mm. Two quartz windows were attached to function as the front/rear walls and to

provide visual access to the combustor section.

An acoustic driver with a maximum power of 75 W was used at the bottom of the model combustor to supply a pressure wave into the premixed flow at the open end of the inlet section. Sine waves, which were generated from a NI VirtualBench and amplified by an Inkel AX5505, were used to force the driver at controlled frequencies and amplitudes. PCB 101A05 dynamic pressure sensors were flush-mounted at both the inlet and combustor walls to measure the pressure fluctuations. Dynamic pressure signals were amplified by a signal conditioner (PCB Piezotronics, 482A16) and recorded at a rate of 10 kHz by a NI c-DAQ.

A DSLR camera (Samsung GX-10) and an ICCD camera (Andor DH334T-18U-03) were set up at opposite sides to simultaneously capture flame images. A 431.5 ± 5 nm bandpass filter, which includes a CH* chemiluminescence band, was mounted to the lens of the ICCD. For simplicity, the present emission measurements are referred to as direct flame images and CH* chemiluminescence images respectively throughout the paper. The photographs for CH* chemiluminescence were taken at 3 fps by controlling the exposure time of the camera to avoid saturation. The direct flame image was obtained from one long-exposed photograph and the CH* chemiluminescence image was acquired by averaging ten long-exposed photographs to remove any random features associated with turbulence.
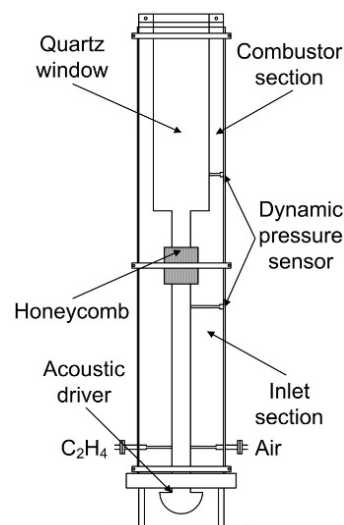

Fig. 1. Schematic of the experimental set-up.

2.2 Test Conditions

Several physical parameters such as the inlet/combustor dimensions, inlet velocity, equivalence ratio, and acoustic forcing frequency/amplitude may affect the flame structure in a dump combustor. In this study, the inlet mean velocity (U), equivalence ratio (φ), forcing frequency (f), and forcing power (Po) were varied independently to investigate their combined effects on the flame length in the dump combustor. To cover a broad turbulent combustion range, the inlet

mean velocity and the equivalence ratio were varied from 7.5 m/s to 12.5 m/s and from 0.55 to 0.80, respectively. The forcing frequency was selected within the range of the jet preferred mode, which in terms of the Strouhal number was between 0.24 and 0.64 (Gutmark and Ho 1983). Considering that the acoustic driver can be operated between 150 and 5,500 Hz, the forcing frequencies were determined differently for each inlet velocity.

In a plane wave, pressure fluctuation (p') and velocity fluctuation (u') are in phase and have a following relation:

$$u' = \frac{p'}{\rho c} \qquad (1)$$

where ρ is a density and c is a speed of sound (Dowling and Williams 1983, Altay 2005, Altay *et al.* 2009a). By detecting pressure fluctuation from the inlet dynamic pressure sensor, the acoustic forcing power was controlled to maintain the normalized inlet velocity peak fluctuation (u_p'/U) constant from 0.1 to 0.5. The test conditions, which include the values of non-dimensional parameters, are summarized in Table 1.

The Reynolds number, Strouhal number, and Damköhler number are defined as follows:

$$\text{Re} = \frac{UW_I}{\nu}, \text{St} = \frac{fW_I}{U}, \text{Da} = \frac{\tau_{flow}}{\tau_{chem}} \qquad (2)$$

where W_I is the inlet width and ν is the kinematic viscosity of air at 298.15 K. Following Ahn and Yu (2012), the characteristic flow time, τ_{flow}, was selected as the period of the forcing frequency. This was because the period of oscillation in unsteady combustion was thought to be reasonable as the characteristic flow time. The characteristic chemistry time, τ_{chem}, was also calculated by dividing the flame thickness by the laminar burning velocity. This followed the process of Sterling (1987), where the laminar burning velocity and flame thickness of lean ethylene flames were acquired from an analytical equation suggested by Göttgens *et al.* (1992).

Table 1 Experimental conditions

U	7.5 m/s	10.0 m/s	12.5 m/s
φ	0.55, 0.60, 0.65, 0.70, 0.75, 0.80		
f	180 Hz	180, 240 Hz	180, 240, 300 Hz
u_p'/U	0.1, 0.2, 0.3, 0.4, 0.5		
Re	1.19×10^4	1.59×10^4	1.99×10^4
St	0.60	0.45, 0.60	0.36, 0.48, 0.60
Da	2.25 ~ 12.45	1.69 ~ 12.45	1.35 ~ 12.45

3. RESULTS AND DISCUSSION

3.1 Flame Images During Acoustic Forcing

Representative images of the direct flame and CH* chemiluminescence data for the case of $U = 10$ m/s, with or without acoustic forcing of $f = 180$ Hz and $Po = 25$ W, are shown in Fig. 2. Figure 2 represents the effects of acoustic forcing and the equivalence

ratio on turbulent premixed flames. These images were taken from an area of 75×215 mm, which was bounded by the two side walls and the inlet dump plane at the bottom. As the equivalence ratio was changed from 0.55 to 0.80 in fuel-lean conditions, the flame became short and intense in the near field of the combustor. Acoustic forcing generated a large periodic vortex structure, which caused the flame to change from a conical shape to a shape with brilliant luminosity in the center and side walls of the combustor. This also made the flame become shorter at relatively low equivalence ratios.
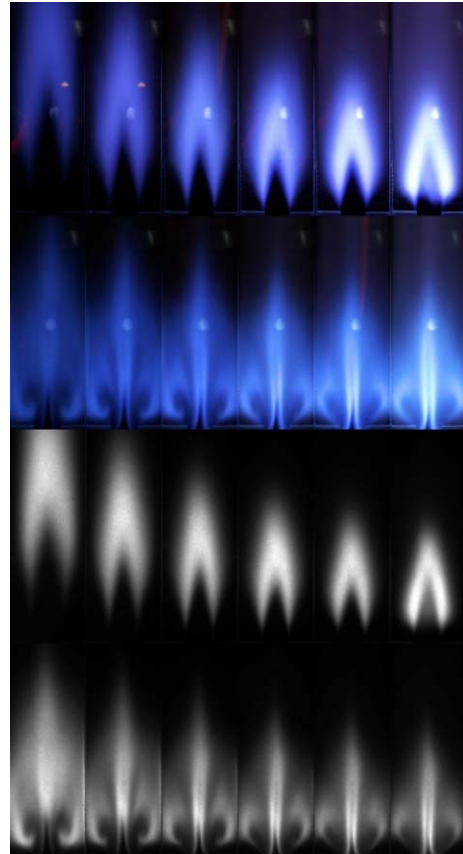

Fig. 2. Flame images at various equivalence ratios (from left to right: φ = 0.55, 0.60, 0.65, 0.70, 0.75, 0.80 and from top to bottom: direct flame images without acoustic forcing, direct flame images with acoustic forcing, CH* chemiluminescence images without acoustic forcing, CH* chemiluminescence images with acoustic forcing) at $U = 10$ m/s.

The radiation intensity of free radicals such as C_2, CH, and OH has been used to measure the rate of combustion. Hurle *et al.* (1968) found that light emission of CH radicals in an ethylene/air flame had a linear relationship with the fuel flow rate for a given equivalence ratio. The relationship between chemiluminescence and the heat release rate was assumed to be linear (Poinsot *et al.* 1987; Langhorne 1988). CH* chemiluminescence has been successfully used previously as a qualitative/quantitative marker for reaction dynamics (Lieuwen and Yang 2005; Altay *et al.*

2009b). Though both the direct flame image and CH* chemiluminescence image had almost the same results as shown in Fig. 2, the direct images included a hazy plume downstream of the bright flame in high equivalence ratios. The flame length and flame center length is therefore calculated from the CH* chemiluminescence image throughout this paper.

3.2 Effects of the Equivalence Ratio, Inlet Velocity, and Acoustic Forcing

Figure 3 shows a sequence of the image processing which was applied to the CH* chemiluminescence images with and without acoustic forcing. To reduce the background noise, a CH* chemiluminescence image averaged from ten photographs was normalized by linearly replacing the maximum intensity value with 255 and the minimum with 0. The normalized image was binarized by substituting pixels with values below 10% of the maximum intensity value with 0 and others with 1. The flame length (L_F) was determined as the maximum height with five sequential 1s in a row in the binarized image. The final image was obtained by multiplying the values at each pixel of the normalized image and the binarized image. The flame center length (L_{FC}) was defined as the height with the maximum value in the sums of each row of pixels in the final image.
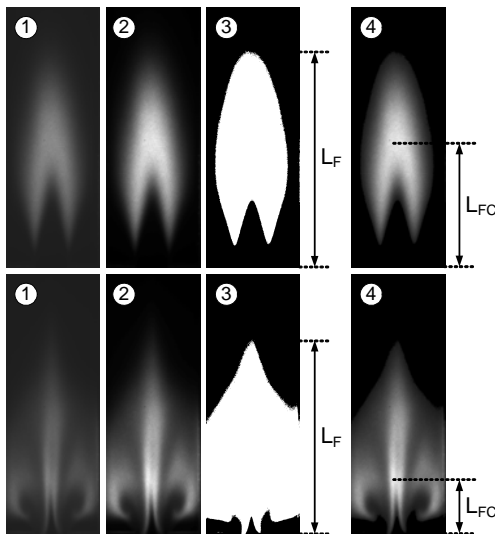

Fig. 3. Sequence of the image processing and definition of the flame length/flame center length for images without and with acoustic forcing (① the averaged CH* chemiluminescence image, ② the normalized image, ③ the binarized image, ④ the final image).

The experimental data of the flame lengths and flame center lengths normalized by the inlet width at f = 300 Hz and U = 12.5 m/s are plotted in Figs. 4 and 5. As could be expected from Fig. 2 and as is shown in Fig. 4, several flame lengths could not be obtained for cases with very low equivalence ratios and especially cases without acoustic forcing, since the flame extended over the measurement window. Nevertheless, the experimental tendency could be

sufficiently acquired due to broad test conditions. As is well known, both flame lengths and flame center lengths decreased with increment of the equivalence ratio in fuel-lean conditions due to shorter chemical reaction time even without acoustic forcing. An increase in the normalized inlet velocity fluctuation generally appeared to cause the flame length and flame center length to be reduced because the considerable burned product was induced to recirculate into the inlet plane and to be rapidly mixed with the fresh premixed gas. It also more strongly affect those with low equivalence ratios, where the early mixing effect of the burned product and fresh reactant by vortical roll-ups was more significantly impacted due to the longer chemical time. It seems that acoustic forcing influenced the flame center lengths greater than the flame length. This could mean that the vortex structure generated by acoustic forcing significantly distorted the flame pattern in the near field of the combustor and became weak in the far field due to the interaction with the flow and combustion.
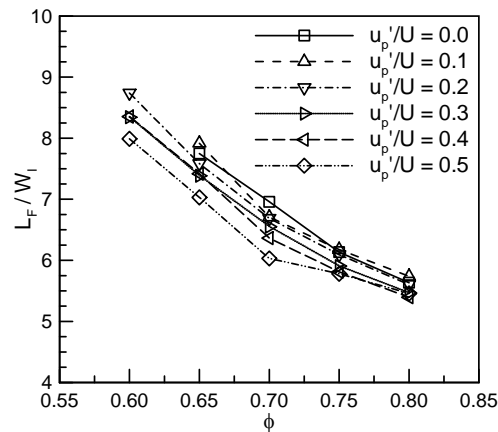

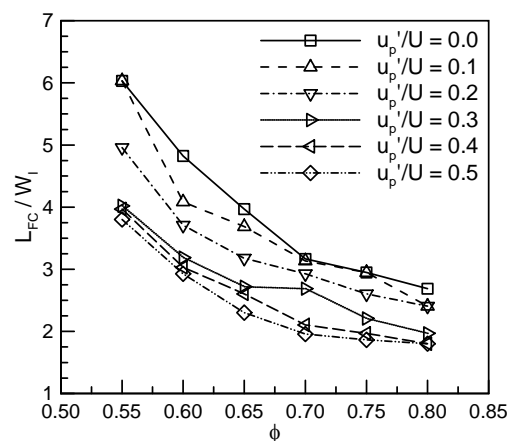**Fig. 4. Effect of the acoustic forcing power on flame lengths in the case of f = 300 Hz and U = 12.5 m/s.**

Fig. 5. Effect of the acoustic forcing power on flame center lengths in the case of f = 300 Hz and U = 12.5 m/s.

Figures 6 and 7 show the effects of inlet velocity on flame lengths and flame center lengths under acoustic forcing at f = 180 Hz and u_p'/U = 0.5. At the same equivalence ratio, as the inlet velocity

decreased, the flame lengths and flame center lengths generally dropped off as reported in gas turbine model combustors (Stöhr *et al.* 2012; Stöhr *et al.* 2013). It is interesting that the difference in the flame lengths was greater than that in the flame center lengths. The reason for this is thought to be that the reaction was most active in the near field due to the vortex roll-up and merging of the two mixing layers and therefore the flame center length was less affected by variation of the inlet velocity. At high equivalence ratios and high inlet velocities, variation in flame center lengths was less owing to near saturation of the recirculation zone length and the reaction time scale. This is similar to the results of Kim *et al.* (2009b) which showed that the flame length did not change when hydrogen was injected above a certain level compared to natural gas.
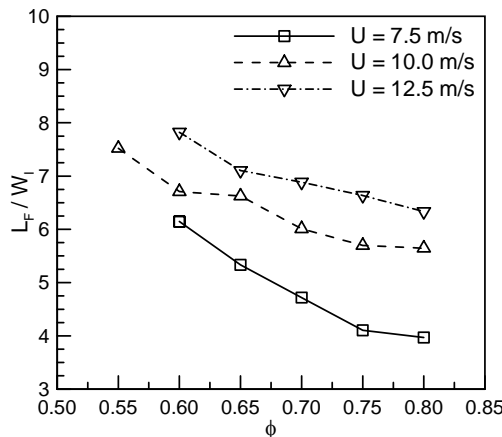

Fig. 6. Effect of the inlet velocity on flame lengths in the case of f = 180 Hz and u_p'/U = 0.5.
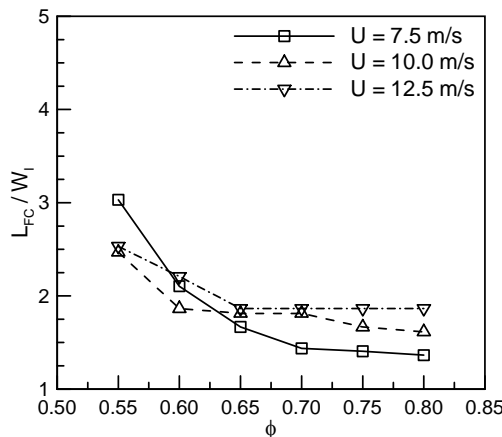

Fig. 7. Effect of the inlet velocity on flame center lengths in the case of f = 180 Hz and u_p'/U = 0.5.

Finally, the influences of the acoustic forcing frequency on the flame lengths and flame center lengths were investigated. The experimental data with respect to the forcing frequency for the case of U = 12.5 m/s and u_p'/U = 0.4 are presented in Figs. 8 and 9. The acoustic forcing frequency played a different role on flame lengths and flame center lengths. As the forcing frequency increased from 180 Hz to 300 Hz, the flame center length generally increased but the flame length showed an opposite

trend. Because the vortical structure size was affected by the acoustic forcing frequency and inlet velocity, the lower forcing frequency at the same inlet velocity was thought to induce larger roll-up structures and to have a locally higher heat release region in the near field of the combustor. It is known that the shear layer has a smaller length scale, whereas the wake has a larger length scale comparable to the extent of dump. The disparity between the flame length and the flame center length could be a result of this scale mismatch.
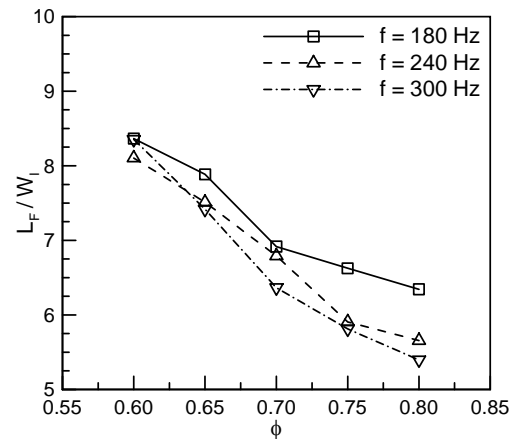

Fig. 8. Effect of the acoustic forcing frequency on flame lengths in the case of U = 12.5 m/s and u_p'/U = 0.4.
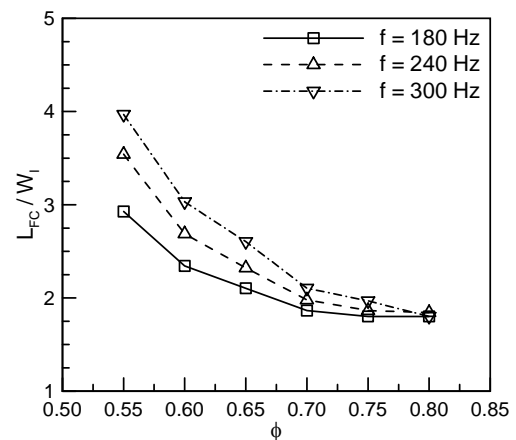

Fig. 9. Effect of the acoustic forcing frequency on flame center lengths in the case of U = 12.5 m/s and u_p'/U = 0.4.

3.3 Effects of the Reynolds Number, Strouhal Number, Damköhler Number, and Normalized inlet Velocity fluctuation

The effects of the equivalence ratio, inlet velocity, and acoustic forcing frequency/amplitude on the flame lengths and flame center lengths in a dump combustor have been examined in the previous section. However, parameters such as the equivalence ratio, inlet velocity, and acoustic forcing frequency/amplitude have dimensions. If one uses a different fuel or a different size of combustor to repeat a similar study, the result may be different. Therefore, the dimensional parameters

were replaced with non-dimensional parameters such as the Reynolds number, Strouhal number, and Damköhler number, which consider the fuel properties and inlet dimensions.

The flame lengths and flame center lengths normalized by the inlet width from the experiment were investigated as functions of the four parameters. The normalized lengths were analyzed on the following assumption:

$$\frac{L}{W_I} = a \times Re^\alpha \times St^\beta \times Da^\gamma \times \left(\frac{u_p'}{U}\right)^\delta \qquad (3)$$

By using multiple linear regression analysis, the variables in the equation were calculated and the following empirical equations were obtained.

$$L_F/W_I = 1.9303 \times Re^{0.1466} \times St^{-0.5100} \times Da^{-0.3643} \times (u_p'/U)^{-0.0404} \qquad (4)$$

$$L_{FC}/W_I = 2.1334 \times Re^{0.0326} \times St^{-0.2281} \times Da^{-0.4404} \times (u_p'/U)^{-0.2943} \qquad (5)$$

The experimental data are plotted with the calculated data in Fig. 10 and 11. The empirical equations are found to match well with the experimental results in the whole range of experimental conditions. From the empirical equations, the following general conclusions can be obtained: 1) as the Reynolds number increased, the flame length and flame center length increased, 2) as the Strouhal number, Damköhler number and normalized inlet velocity fluctuation increased, the flame length and flame center length decreased.
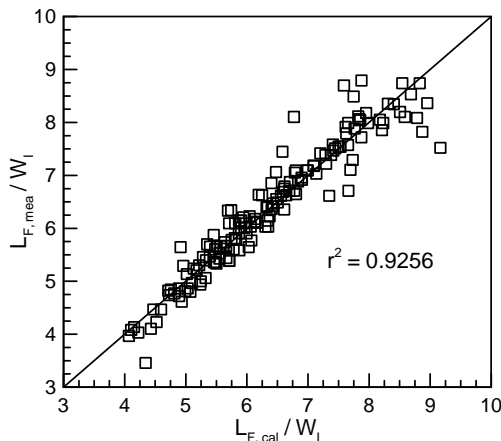

Fig. 10. Comparison of the measured flame length data with those estimated from Eq. (4).

4. SUMMARY AND CONCLUSIONS

Flame lengths and flame center lengths of premixed flames in a dump combustor simulating unstable combustion were experimentally investigated. Experiments using ethylene and air were performed, changing the inlet velocity, equivalence ratio, and acoustic forcing power/frequency. For a more general finding, the flame length and flame center length were normalized by the inlet width. The dimensional operating parameters were replaced with non-dimensional parameters such as the Reynolds number, Strouhal number, Damköhler

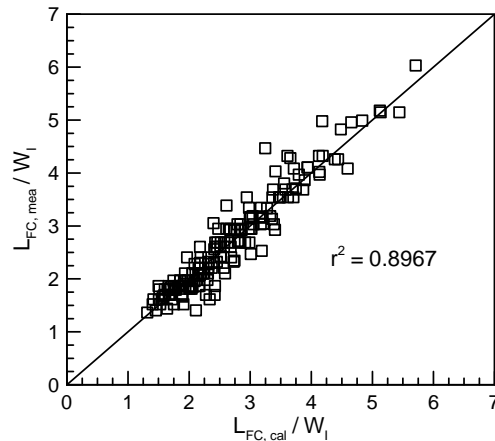number, and normalized inlet velocity fluctuation.

Fig. 11. Comparison of the measured flame center length data with those estimated from Eq. (5).

Acoustic forcing affected more significantly heat release rate in the near field of the combustor under relatively low equivalence ratios. As the inlet velocity decreased and the equivalence ratio increased, the flame lengths and flame center lengths generally became shorter. The acoustic forcing frequency played a different role on the flame lengths and flame center lengths.

The flame lengths and flame center lengths normalized by the inlet width could be expressed well as a function of non-dimensional parameters. It was found that an increase in the Reynolds number and a decrease in the Damköhler number, Strouhal number and normalized inlet velocity fluctuation caused the flame length/flame center length to become greater. In light of these findings, one could expect a flame pattern in unstable combustion if one knows the non-dimensional parameters.

As a first step, ethylene with wide combustion limits and a low ignition temperature/energy was used in this study. Though the present results in a dump combustor shed new insight into the flame pattern in unstable combustion, more general validity of the results using other fuels with a low reactivity is highly recommended to achieve a deeper understanding. Also, the phase-averaged flame length/flame center length with respect to different acoustic pressure phases will be carried out for future work.

ACKNOWLEDGEMENTS

REFERENCES

Ahn, K. (2014). Effect of combustion instability on

heat transfer in a subscale thrust chamber. *Journal of the Korea Academia-Industrial Cooperation Society* 15(6), 3403-3409.

Ahn, K. and K. H. Yu (2012). Effects of Damköhler number on vortex-flame interaction. *Combustion and Flame* 159(2), 686-696.

Ahn, K., B. Lim and H. S. Choi (2014). Stability characteristics of bi-swirl coaxial injectors in fuel-rich combustion. *Transactions of the Japan Society for Aeronautical and Space Sciences* 57(6), 317-324.

Altay (2005). *Vortex Driven Flame Dynamics and Combustion Instability.* Master thesis, Massachusetts Institute of Technology, Massachusetts, U.S.A.

Altay, H. M., R. L. Speth, D. E. Hudgins and A. F. Ghoniem (2009a). Flame-vortex interaction driven combustion dynamics in a backward-facing step combustor. *Combustion and Flame* 156(5), 1111-1125.

Altay, H. M., R. L. Speth, D. E. Hudgins and A. F. Ghoniem (2009b). The impact of equivalence ratio oscillations on combustion dynamics in a backward-facing step combustor. *Combustion and Flame* 156(11), 2106-2116.

Bondaryuk, M. N. and S. M. Il'yashenko (1960, February). *Ramjet Engines.* Wright-Patterson Air Force Base, U.S.A.

Buchner, H., C. Hirsch and W. Leuckel (1993). Experimental investigation on the dynamics of pulsated premixed axial jet flames. *Combustion Science and Technology* 94(1), 219-228.

Byrne, R. W. (1983). Longitudinal pressure oscillations in ramjet combustor. In *Proceedings of the 19th Joint Propulsion Conference*, Seattle, Washington, U.S.A.

Choi, B. C. and H. T. Kim (2002). Comparison of theoretically and experimentally determined simulated coal syngas turbulent jet flame lengths. *Journal of Industrial and Engineering Chemistry* 8(6), 578-585.

Dahm, W. J. A. and A. G. Mayman (1990). Blowout limits of turbulent jet diffusion flames for arbitrary source conditions. *AIAA Journal* 28(7), 1157-1162.

Dhanuka, S. K., J. E. Temme and J. F. Driscoll (2011). Lean-limit combustion instabilities of a lean premixed prevaporized gas turbine combustor. *Proceedings of the Combustion Institute* 33(2), 2961-2966.

Dowling, A. P. and J. E. F. Williams (1983). *Sound and Sources of Sound.* John Wiley & Sons, New York, U.S.A.

Foglesong, R. E., T. R. Frazier, L. M. Flamand, J. E. Peters and R. P. Lucht (1999). Flame structure and emissions characteristics of a lean premixed gas turbine combustor. In *Proceedings of the 35th Joint Propulsion Conference and Exhibit,* Los Angeles, California, U.S.A.

Ghoniem, A. F. and G. Heidarinejad (1991). Effect of Damköhler number on the reactive zone structure in a shear layer. *Combustion and Flame* 83(1), 1-16.

Göttgens, J., F. Mauss and N. Peters (1992). Analytic approximations of burning velocities and flame thickness of lean hydrogen, methane, ethylene, ethane, acetylene, and propane flames. *Proceedings of the Combustion Institute* 24(1), 129-135.

Gutmark, E. and C. M. Ho (1983). Preferred modes and the spreading rates of jets. *Physics of Fluids* 26(10), 2932-2938.

Hill, P. G. and C. R. Peterson (1992). *Mechanics and Thermodynamics of Propulsion.* 2nd ed. Addison-Wesley.

Hurle, I. R., R. B. Price, T. M. Sugden and A. Thomas (1968). Sound emission from open turbulent premixed flames. *Proceedings of the Royal Society* 303(1475), 409-427.

Kim, K. T. and D. Santavicca (2009). Linear stability analysis of acoustically driven pressure oscillations in a lean premixed gas turbine combustor. *Journal of Mechanical Science and Technology* 23(12), 3436-3447.

Kim, K. T., J. G. Lee, H. J. Lee, B. D. Quay and D. Santavicca (2009b). Characterization of forced flame response of swirl-stabilized turbulent lean-premixed flames in a gas turbine combustor. *Proceedings of ASME Turbo Expo*, Orlando, Florida, U.S.A.

Kim, M., Y. Choi, J. Oh and Y. Yoon (2009a). Flame-vortex interaction and mixing behaviors of turbulent non-premixed jet flames under acoustic forcing. *Combustion and Flame* 156(12), 2252-2263.

Langhorne, P. J. (1988). Reheat buzz: an acoustically coupled combustion instability. part 1. experiment. *Journal of Fluid Mechanics* 193, 417-443.

Lefebvre, A. W. (1977). *Lean Premixed/prevaporized Combustion.* NASA Lewis Research Center, U.S.A.

Lieuwen, T. C. and V. Yang (2005). *Combustion Instabilities in Gas Turbine Engines: Operational Experience, Fundamental Mechanisms, and Modeling.* AIAA, Reston, U.S.A.

Morcos, V. H. and Y. M. Abdel-Rahim (1999). Parametric study of flame length characteristics in straight and swirl light-fuel oil burners. *Fuel* 78(8), 979-985.

Poinsot, T. J., A. C. Trouve, D. P. Veynante, S. M. Candel and E. J. Esposito (1987). Vortex-driven acoustically coupled combustion instabilities. *Journal of Fluid Mechanics* 177, 265-292.

Renard, P. H., D. Thévenin, J. C. Rolon, and S. M. Candel (2000). Dynamics of flame/vortex interactions. *Progress in Energy and Combustion Science* 26(3), 225-282.

Rutland, C. J. and J. H. Ferziger (1991). Simulations of flame-vortex interactions. *Combustion and Flame* 84(3), 343-360.

Sterling, J. D. (1987). *Longitudinal Mode Combustion Instabilities in Air Breathing Engines.* Ph. D. thesis, California Institute of Technology, California, U.S.A.

Stöhr, M., C. M. Arndt and W. Meier (2013). Effects of Damköhler number on vortex-flame interaction in a gas turbine model combustor. *Proceedings of the Combustion Institute* 34(2), 3107-3115.

Stöhr, M., I. Boxx, C. D. Carter and W. Meier (2012). Experimental study of vortex-flame interaction in a gas turbine model combustor. *Combustion and Flame 159*(8), 2636-2649.

Turns, S. R. (2012). *An Introduction to Combustion: Concepts and Applications. 3rd ed.* McGraw-Hill, New York, U.S.A.

Yu, K. H., A. Trouve and J. W. Daily (1991). Low-frequency pressure oscillations in a model ramjet combustor. *Journal of Fluid Mechanics* 232, 47-72.